October 2000 • NREL/CP-520-29064

Conference Paper

Studies of Band Structure and Free-Carrier Scattering in Transparent Conducting Oxides Based on Combined Measurements of Electron Transport Phenomena

V.I. Kaydanov
Colorado School of Mines

T.J. Coutts and D.L. Young
National Renewable Energy Laboratory

Presented at the Material Research Society Workshop
Denver, Colorado
June 19–20, 2000

National Renewable Energy Laboratory

1617 Cole Boulevard
Golden, Colorado 80401-3393

NREL is a U.S. Department of Energy Laboratory
Operated by Midwest Research Institute • Battelle • Bechtel

Contract No. DE-AC36-99GO10337

NOTICE

The submitted manuscript has been offered by an employee of the Midwest Research Institute (MRI), a contractor of the US Government under Contract No. DE-AC36-99GO10337. Accordingly, the US Government and MRI retain a nonexclusive royalty-free license to publish or reproduce the published form of this contribution, or allow others to do so, for US Government purposes.

This report was prepared as an account of work sponsored by an agency of the United States government. Neither the United States government nor any agency thereof, nor any of their employees, makes any warranty, express or implied, or assumes any legal liability or responsibility for the accuracy, completeness, or usefulness of any information, apparatus, product, or process disclosed, or represents that its use would not infringe privately owned rights. Reference herein to any specific commercial product, process, or service by trade name, trademark, manufacturer, or otherwise does not necessarily constitute or imply its endorsement, recommendation, or favoring by the United States government or any agency thereof. The views and opinions of authors expressed herein do not necessarily state or reflect those of the United States government or any agency thereof.

Available electronically at http://www.doe.gov/bridge

Available for a processing fee to U.S. Department of Energy and its contractors, in paper, from:

U.S. Department of Energy
Office of Scientific and Technical Information
P.O. Box 62
Oak Ridge, TN 37831-0062
phone: 865.576.8401
fax: 865.576.5728
email: reports@adonis.osti.gov

Available for sale to the public, in paper, from:

U.S. Department of Commerce
National Technical Information Service
5285 Port Royal Road
Springfield, VA 22161
phone: 800.553.6847
fax: 703.605.6900
email: orders@ntis.fedworld.gov
online ordering: http://www.ntis.gov/ordering.htm

Printed on paper containing at least 50% wastepaper, including 20% postconsumer waste

Studies of Band Structure and Free-Carrier Scattering in Transparent Conducting Oxides Based on Combined Measurements of Electron Transport Phenomena

V.I. Kaydanov,[1] T.J. Coutts,[2] and D.L. Young[2]

[1]Colorado School of Mines, Golden, CO 80401
[2]National Renewable Energy Laboratory, 1617 Cole Blvd., Golden, CO 80401

Abstract

Experimental methods are discussed for studying band structure, effective mass, and other electronic properties relevant to mobility, including scattering mechanisms, relaxation time, and the influence of grain boundaries (GBs) in polycrystalline transparent conducting oxide (TCO) films. Optical characterization (ultra-high-frequency transport) gives the conductivity effective mass, m_c*, and relaxation time, τ, and, hence, the optical mobility, $\mu_0 = e\tau / m_c^*$, derived from the plasma and collision frequencies. Combined measurements of resistivity (ρ), Hall (R_H), Seebeck, and Nernst-Ettingshausen coefficients (transport in constant external fields) provide the density-of-states effective mass, m_d^*, scattering parameter, s, which reveals the dominating scattering mechanism, and Hall mobility, $\mu_H = R_H / \rho$. Comparison of m_d^* with m_c^* provides guidance about the shape of the constant-energy surfaces. The dependence of m_c^* and m_d^* on carrier concentration/Fermi level position is used for studying the band shape and the dependence of electron energy on its wave vector. Comparison of μ_H and μ_o provides information about the role of GBs in modifying the resistivity of polycrystalline films. Impedance spectroscopy permits evaluation of the GB potential barrier height and density-of-states. These studies enable an estimate of the limiting mobility achievable for practical transparent conducting oxides to be made. The equipment for measurement of the four transport coefficients is discussed, and examples of its application to films of ZnO, SnO_2, and Cd_2SnO_4 are given.

1. Introduction

To improve the properties of existing and new transparent conducting oxides (TCOs), it is important to put the topic on a solid scientific basis by obtaining detailed information about the electronic properties of thin films, as well as about the effect of substrates (glass, polymer, other semiconductors), film structure, and morphology etc.

This information, and its theoretical analysis, will enable an estimate to be made of the limiting mobility and of the achievable figure-of-merit for practical TCOs. The approach requires a wide variety of analytical tools for the characterization of thin films and a detailed understanding of the physics and chemistry of the materials needed to interpret the data.

In this paper, we discuss several experimental methods used to study the electronic band structure and the dominant electron scattering mechanism(s) in TCOs and similar materials. These methods are based on measurements of electron transport phenomena and may be applied to single crystals, as well as to polycrystalline thin films. When studying polycrystalline thin films, we usually face an important problem, which is to elucidate the influence of the grain boundaries on electrical properties and, in particular, on the measured film sheet resistance and bulk resistivity. We need to determine and compare the relative magnitudes of inter- and intra-grain scattering when calculating the upper limit of mobility in the film. For this reason, we discuss two methods used to study the electrical properties of grain boundaries.

In section 2, we discuss the electronic properties that determine carrier mobility and affect the optical transmittance. These are primarily the effective mass and the nature of carrier scattering processes. In the third section, we discuss a novel method to measure these quantities that depends on the measurement of four electron-transport coefficients: the electrical resistivity and the Hall, Seebeck and Nernst-Ettingshausen coefficients.[1] The method, known as *the method of four coefficients*, enables us to determine the carrier mobility (Hall mobility), the density-of-states effective mass, relaxation time, and scattering parameter, which indicates the nature of the dominant scattering mechanism.

Optical characterization (ultra-high-frequency transport) is discussed in section 4. This method is based on measurements of plasma and collision frequencies. The first of these provides the value of the conductivity effective mass, and the latter gives the collision frequency (relaxation time). From these data, the optical mobility also can be calculated.

Two methods used to evaluate the contribution of grain boundaries to the resistivity and to study the specific electronic properties of the grain boundaries are discussed in section 5. One of these is based on a simple comparison of the Hall and optical mobilities. The other method, which is suitable for polycrystalline material with semi-insulating grain boundaries, is based on impedance spectroscopy. The equipment for measurement of the four transport coefficients is discussed, and some results on films of ZnO, SnO_2, and Cd_2SnO_4 are given in sections 6 and 7.

2. Electron parameters to be determined and their influence on film properties

2.1 Band model, the effective mass tensor, density of states

Along with the bandgap that defines the short-wavelength transmission limit of the material, other details of the band structure are necessary to determine the achievable figure-of-merit. In general, we need to know the dependence of the carrier energy on its wave vector, $\boldsymbol{k}$, in the conduction band. In particular, we are interested in the shape of the constant-energy surfaces in $\boldsymbol{k}$-space and the effective mass, which is equivalent to the

dependence $E(\boldsymbol{k})$. We will limit the discussion to i) isotropic, spherically shaped surfaces, ii) single-ellipsoid surfaces, and iii) multi-ellipsoid surfaces. By way of example, we shall consider the conduction band of silicon.

In general, the reciprocal effective mass is a second-rank tensor that reduces to a scalar quantity for a spherical band. For an ellipsoidal surface, it is characterized by three values of effective mass, m_i^* (i=1, 2, 3), each corresponding to one of the principal axes of the ellipsoid.[2]

In the case of the ellipsoid of revolution, we have only two independent values of the effective mass: $m_{\|}^*$ related to the direction of the revolution axis, and $m_{\perp}^*$ related to the perpendicular axis. In the n-Si-like band model, we have six equivalent ellipsoids located in $\boldsymbol{k}$-space on the [100]-type axes, which are the axes of revolution.

Together with the relaxation time, τ, which is to the first approximation the reciprocal of the collision (scattering) frequency, effective mass determines mobility: the smaller the effective mass, the higher the mobility. For the isotropic band, the carrier mobility is determined by the equation

$$\mu = \frac{e\langle\tau(E)\rangle}{m^*}, \tag{2.1}$$

in which $\langle\tau(E)\rangle$ symbolizes averaging τ over the conduction band, weighted by $E^{3/2}\frac{\partial f_0}{\partial E}$, where f_0(E) is the Fermi-Dirac distribution function. A highly degenerate electron gas, such as a typical TCO, has $(E_F - E_c)/k_BT >> 1$. E_F is Fermi energy, E_c is the energy of the minimum in the conduction band, both being referenced to the vacuum or some other energy level, and k_B is the Boltzmann constant. In such materials, only carriers with energies close to the Fermi level contribute to electron transport. The properties of these carriers determine the magnitude of the mobility and the other transport coefficients. Thus, for an isotropic band, mobility is given by

$$\mu = e\,\tau(E_F)/m^*(E_F). \tag{2.2}$$

Subsequently, we shall presume high degeneracy and omit the reference to the Fermi level. For an isotropic relaxation time, the only reason for the mobility to be anisotropic is anisotropy of the effective mass. For a single ellipsoidal band, the mobility may be expressed as

$$\mu_i = e\,\tau/m_i^*, \tag{2.3}$$

in which the subscript refers to the three principal axes. In polycrystalline material, with randomly oriented crystallites, averaging spatially leads to an isotropic mobility given by

$$\mu = \frac{1}{3} e \tau \sum_{i=1}^{3} \frac{1}{m_i^*} . \tag{2.4}$$

For crystals of cubic symmetry with multi-valleys, such as n-Si or n-Ge, the mobility is isotropic and may be described by

$$\mu = e \tau / m_c^* . \tag{2.5}$$

m_c^* is the *conductivity effective mass* and is determined by:[2]

$$\frac{1}{m_c^*} = \frac{1}{3}\left(\frac{1}{m_{\|}^*} + \frac{2}{m_{\perp}^*} \right) . \tag{2.6}$$

The reciprocal mass given by equation (2.6) is a weighted average of the three individual reciprocal masses. The factor of 2 inside the parentheses arises because there is rotational symmetry of the ellipsoid in ***k***-space. The conductivity effective mass influences the plasma frequency and, hence, the long-wave limit of transparency of the TCO. The plasma frequency is given by

$$\omega_p = \left(\frac{e^2 n}{m_c^* \varepsilon_\infty \varepsilon_0} \right)^{1/2} , \tag{2.7}$$

where n is the carrier concentration, ε_0 is the free-space dielectric constant, and ε_∞ is the high frequency dielectric permittivity of the material.

The density-of-states (DOS) function, $D(E)$, is an important property of a material that also depends on effective mass. For a parabolic band spectrum ($E \propto k^2$),

$$D(E) = \frac{4\pi \left(2 m_d^*\right)^{3/2}}{h^3} E^{1/2} . \tag{2.8}$$

Here, m_d^* is the DOS effective mass, which is a combination of the effective-mass components. For the cases of an isotropic spectrum, a single ellipsoid band and a multi-ellipsoidal band, the DOS effective mass is given by equations 2.9 a), 2.9 b), and 2.9 c), respectively.

$$m_d^* = m^* \qquad \text{a)}$$
$$m_d^* = \left(m_1^* m_2^* m_3^*\right)^{1/3} \qquad \text{b)} \qquad (2.9)$$
$$m_d^* = \mathrm{N}^{2/3}\left(m_1^* m_2^* m_3^*\right)^{1/3}, \qquad \text{c)}$$

where N is the number of the equivalent ellipsoids, e.g., N = 6 for n-Si. It is seen that m_d^* can differ significantly from m_c^*, especially for the multi-ellipsoid model. Comparison of these two values, which may be obtained experimentally, can provide information about the band structure and, in particular, whether it is single- or multi-valley. It can also reveal information about the anisotropy of the constant-energy ellipsoids, i.e., about the ratio $\beta = m_{\|}/m_{\perp}$.

In turn, the DOS function, hence the effective mass, determines the Fermi level for a specific carrier concentration, which is:

$$E_F = \left(\frac{3n}{8\pi}\right)^{2/3}\left(\frac{h^2}{2m_d^*}\right). \qquad (2.10)$$

The change in the position of the Fermi level as a function of carrier concentration, relative to the conduction-band minimum, is the Burstein-Moss shift, which defines the short-wave limit for transparency.[3]

2.2 Carrier scattering, relaxation time, scattering parameter

Carrier scattering leads to a finite mobility value. The higher the scattering (collision) frequency (hence the lower the relaxation time), the lower the mobility. High scattering rate makes the plasma reflection edge less sharp, thus worsening the transparency spectrum. It also affects the absorption by free carriers. Carriers are scattered by phonons, point defects (e.g., vacancies, interstitials, impurity atoms and ions) dislocations, and two-dimensional defects, such as small-angle boundaries (dislocation walls) or grain boundaries in a very fine granular structures. Although the effective mass is considered an intrinsic parameter of a material that depends on its composition, the relaxation time is much influenced by the crystal quality, which depends on structural imperfections and, hence, on the film preparation technique.

Relaxation time depends on the carrier energy, and this dependence is different for different scattering mechanisms. In the case of semi-elastic scattering, dependence of scattering frequency on energy can be presented in the form:

$$\tau^{-1}(E) \propto W(E)D(E), \qquad (2.11)$$

where $D(E)$ is the DOS function and $W(E)$ is the square of the element of electron scattering matrix, which gives the probability of transition from one quantum state to another of the same energy. For the most commonly discussed scattering mechanisms,

theory shows that, in a parabolic band, $W(E)$ is a power function of energy and is commonly represented as

$$W(E) \alpha E^{-r}. \tag{2.12}$$

In a parabolic band, the density of states is given by

$$D(E) \alpha E^{1/2}, \tag{2.13}$$

which means that the dependence of scattering frequency on energy is of the form:

$$\tau \alpha E^{r-1/2}. \tag{2.14}$$

The quantity *r* is known as the scattering parameter, and it is different for each scattering mechanism, varying from $r = 0$ for acoustic phonon scattering, to $r = 2$ for ionized impurity scattering. This kind of dependence, with a fixed value of the scattering parameter, takes place only if the same scattering mechanism dominates over the entire energy range. In reality, several scattering mechanisms of relatively equal importance, may occur simultaneously. The total scattering frequency is the sum of the individual frequencies due to each of the scattering mechanisms, which may be expressed as

$$\omega_c = \tau_c^{-1} = \sum_i \tau_i^{-1}. \tag{2.15}$$

The dependence of relaxation time on energy can be more complicated when a wide range of energies is being considered. Fortunately, in the case of high degeneracy (the only practical case for TCOs), only a narrow range of energy around E_F is of interest. In this case, *W(E)* can be approximated by a power function:

$$W(E) = W(E_F) \times (E/E_F)^{-r}. \tag{2.16}$$

The scattering parameter in this case is defined as

$$r(E_F) = \left(\frac{d \ln \tau}{d \ln E} \right)_{E=E_F} + \frac{1}{2}. \tag{2.17}$$

Along with the concentration and temperature dependence of mobility, knowledge of the scattering parameter value is important for identifying the dominant scattering mechanism(s). It is also to be noted that relaxation time depends on the effective mass because of its inverse dependence on the density of states. In heavily doped (degenerate) TCOs, scattering by impurity ions is sometimes the dominant scattering mechanism. In this case, for materials that have the same carrier concentration, density of electrically active impurity ions, and dielectric permittivity, there can be a difference in mobility because of different effective masses, because $\tau_{ii} \propto 1/m^*$; thus, $\mu_{ii} \propto 1/m^{*2}$.

2.3 Influence of non-parabolicity

The dependence $E(k)$ is parabolic only in the immediate vicinity of the conduction-band minimum. As energy increases, the dependence deviates from parabolic, and the only question is at what energy the deviation becomes sufficiently important to influence the properties of electrons of interest. The most obvious indication of non-parabolicity is the increase of measured effective mass with energy (with Fermi level or carrier concentration in degenerate semiconductors). In narrow-gap, direct-gap semiconductors, such as InSb, (Hg,Cd)Te,[4] PbSe,[5] or PbTe,[6] non-parabolicity significantly affects electronic transport properties at Fermi levels of only $E_F \sim 0.1$ eV, or even lower. For wide-gap semiconductors, such as TCOs, non-parabolicity has not been investigated much, but for heavily doped ZnO and Cd_2SnO_4 with $E_F \sim 0.4$-0.8 eV, it has been established that there is a progressive increase of the DOS effective mass with carrier concentration.[12,14]

To analyze the influence of non-parabolicity in this paper, we consider the theory of electron transport developed by Kolodziejchak et al.[7] and by Zawadzki et al.[8] for the rather general, multi-ellipsoid, non-parabolic band model. The equations for the transport coefficients are based on solutions of the Boltzmann equation and the relaxation time approximation.

In two studies[7,8], the energy dependence on wave vector in the principal ellipsoid axes (1, 2, 3) is described by the equation:

$$\frac{\hbar^2}{2}\left(\frac{k_1^2}{m_{10}^*}+\frac{k_2^2}{m_{20}^*}+\frac{k_3^2}{m_{30}^*}\right)=\gamma(E)=E\left(1+\frac{E}{E_1}+\frac{E^2}{E_2^2}+\frac{E^3}{E_3^3}+\cdots\cdots\right), \tag{2.18}$$

where m_{i0}^* (i=1, 2, 3) are the effective mass components at the bottom of the band (E=0) in the x, y, and z directions. $\gamma(E)$ is an arbitrary function of energy that may be represented as a power series in energy, with coefficients given by E_1, E_2, E_3, etc. The latter have dimensions of energy raised to the same power as their energy term in each numerator. The values of E_1, E_2, E_3, etc., determine the deviation of the spectrum from parabolic for each energy E. If E is much less than each of the coefficients E_1, E_2, E_3, etc. the equation reduces to that of a parabolic band. We will refer to first-order non-parabolicity as the case when

$$\gamma(E)\approx E\left(1+\frac{E}{E_1}\right) \tag{2.19}$$

in the energy range of interest, while the terms of higher in energy power can be neglected.

For the non-parabolic spectrum, the equations for the effective masses, density-of-states function, and carrier concentration are

$$m_i^*(E) = m_{i0}^* \frac{d\gamma}{dE} \qquad \text{a)}$$

$$m_c^*(E) = m_{c0}^* \frac{d\gamma}{dE} \qquad \text{b)} \tag{2.20}$$

$$m_d^*(E) = m_{d0}^* \frac{d\gamma}{dE} \qquad c)$$

$$D(E) = \frac{4\pi\left(2m_{d0}^*\right)^{3/2}}{h^3}\left[\gamma(E_F)\right]^{1/2}\frac{d\gamma}{dE} \tag{2.21}$$

$$n = \frac{8\pi}{3}\frac{\left(2m_{d0}^*\right)^{3/2}}{h^3}\left[\gamma(E_F)\right]^{3/2}. \quad \text{(high degeneracy)} \tag{2.22}$$

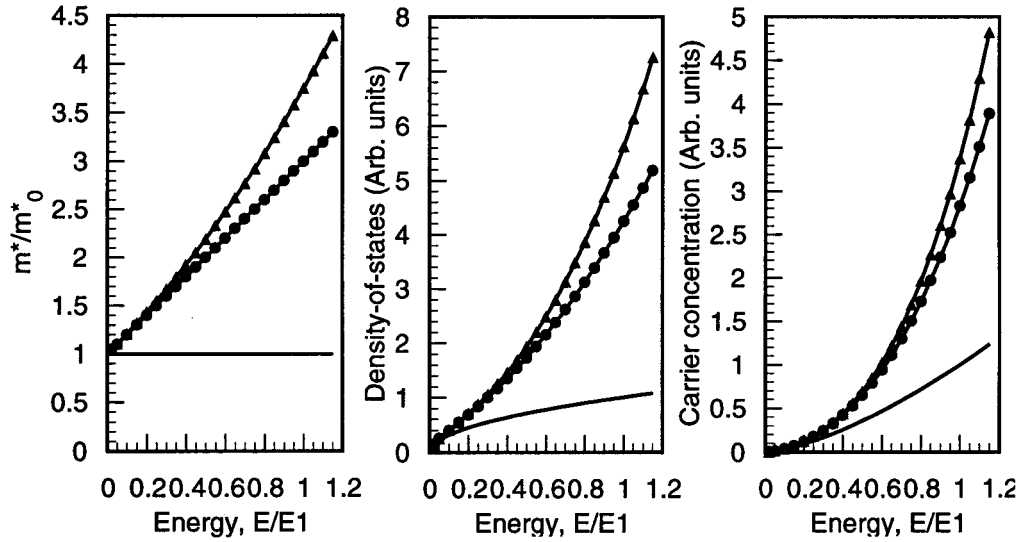

Figure 1. Influence of non-parabolicity on effective mass, density-of-states and carrier concentration. The solid lines in each of the three figures show the variation for a parabolic band, for which $m^*(E) = m_0 = \text{const.}$, $D(E) \alpha E^{1/2}$, and $n \alpha E^{3/2}$. Two cases of non-parabolicity are considered. The symbols ●, indicate first-order non-parabolicity, which is given by $\gamma = E\left(1 + E/E_1\right)$. The ▼ symbols indicate second-order non-parabolicity, which is given by $\gamma = E\,(1 + E/E_1 + E^2/E_2^2)$. In the latter calculation, E_2 was taken as equal to 2 E_1. In both of the non-parabolic band calculations, $m^*(E) = m_0^* d\gamma/dE$, $D(E) \propto \left(m_0^*\right)^{3/2}\left[\gamma(E_F)\right]^{1/2}(d\gamma/dE)$, and $n \propto \left(m_0^*\right)^{3/2}\left[\gamma(E_F)\right]^{3/2}$.

It is seen that the effective mass increases with energy because $d\gamma/dE > 0$. The density of states grows more rapidly with energy and the Fermi level increases slower with the carrier concentration than in a parabolic band. These statements are illustrated in Figure 1.

Non-parabolicity changes the relaxation-time dependence on energy. One of the reasons is the change in the $D(E)$ dependence. The scattering matrix element is preserved with the same dependence as in the parabolic case, $W(E) \propto \left(k^2\right)^{-r}$, with the same values of

the scattering parameter r for each particular scattering mechanism.[7,8] Thus, based on equations (2.16) and (2.21), one obtains for the non-parabolic spectrum,

$$\tau \propto \left[W(E)D(E)\right]^{1} \propto \gamma^{r-1/2}\left[\frac{d\gamma}{dE}\right]^{-1}, \tag{2.23}$$

instead of $\tau \propto E^{r-1/2}$ for the parabolic band.

The above analysis shows that we need to know the real dependence, *E(k)*, when trying to estimate the limiting value of mobility, $\mu_{lim,}$ for heavily doped TCOs. Using, for example, the effective mass obtained from a sample of not-too-high a carrier concentration, one can overestimate μ_{lim} for a material with a more-typical carrier concentration. The same is true for the plasma frequency and the Burstein-Moss shift. Analysis of the transport phenomena, aimed at establishing the dominant scattering mechanism, can lead to the wrong conclusions if parabolic theory is applied to a material with a non-parabolic $E \sim k$ dependence.

3. The Method of Four-Coefficients (Electron Transport in Constant External Fields)

The method discussed in this section is aimed at the determination of mobility, the DOS effective mass, m_d^*, and the scattering parameter, r, in highly degenerate materials, as a function of the carrier concentration/Fermi energy. It is based on the simultaneous measurements of four transport coefficients: electrical conductivity, Hall, Seebeck, and Nernst-Ettingshausen coefficients, σ, R_H, α, and Q, respectively. The method does not require fulfilling the condition of strong magnetic field (μB>>1), as do some powerful methods (e.g., cyclotron resonance, Shubnikov-de Haas) for band-structure studies. This is a significant advantage for TCOs because they typically have small mobilities and do not meet this condition (μ<100 cm^2 V^{-1} s^{-1}, and $\mu B \sim 0.01$ for B = 1 tesla).

Hall effect measurements provide the carrier concentration. In a weak magnetic field ($\mu B << 1$),

$$R_H = A_R/qn, \tag{3.1}$$

where $q = -e$ for electrons and $q = e$ for holes. The *Hall factor, A_R,* which is isotropic for spherical and single-ellipsoid constant-energy surfaces, is very close to 1 in the case of high degeneracy. For a multi-ellipsoid band in cubic crystals (like n-Si and n-Ge), it is also isotropic, but its value depends on the anisotropy of the ellipsoids. It is given by[2,4]

$$A_R = \frac{3\beta(\beta+2)}{(2\beta+1)^2}, \tag{3.2}$$

where

$$\beta = \frac{m_{\parallel}}{m_{\perp}}. \tag{3.3}$$

This brings some uncertainty in the determination of n but, fortunately, this is small for typical materials. For example, $A_R = 0.82$ for $\beta = 10$. However, a more realistic value of $\beta = 2$, $A_R = 0.96$. Combined measurements of σ and R_H provide an estimate of the mobility. The so-called Hall mobility, μ_H, differs from the real drift mobility, μ, by the Hall factor, A_R. Hence,

$$\mu_H = |R_H|\sigma = A_R \mu. \tag{3.4}$$

Combined measurement of Hall coefficient (carrier concentration) and Seebeck coefficient (thermopower) is one of the oldest methods used to estimate the effective mass in semiconductors. For a parabolic band and high degeneracy,[2,4] the Seebeck coefficient is given by

$$\alpha = 8\pi\left(\frac{\pi}{3}\right)^{5/3} \frac{k_B^2 T}{q h^2}(r+1)\frac{m_d^*}{n^{2/3}}. \tag{3.5}$$

Equation (3.5) contains one more quantity to be determined, namely, the *scattering parameter*, r. Using equation (3.5), without knowledge of the value of the scattering parameter, can lead to a rather inaccurate estimate of m_d^*. For example, if one assumes that the dominant scattering mechanism is due to acoustic phonons, for which r=0, one will obtain a value of m_d^* three times greater than that obtained if one assumes ionized impurity scattering, for which $r = 2$.

The problem can be solved by measuring the conductivity and the transverse Nernst-Ettingshausen (N-E) coefficient, in addition to the Hall and Seebeck coefficients. The thermomagnetic N-E effect is defined by the equation[1]

$$E_y = -Q\frac{dT}{dx}B_z. \tag{3.6}$$

For a parabolic band and with high degeneracy of the carrier gas, the N-E coefficient, Q, can be described by

$$Q = |\alpha|\mu_H \frac{r - 1/2}{r+1}. \tag{3.7}$$

Combining equations (3.5) and (3.6), one obtains

$$m_d^*(E_F) = \left(\frac{3N}{8\pi^4}\right)^{2/3} \frac{e\,h^2}{k_B^2 T}\left(|\alpha| - \frac{Q}{\mu_H}\right), \tag{3.8}$$

and

$$r = \frac{3}{2}\left(\frac{Q}{|\alpha|\mu_H - Q}\right) + \frac{1}{2}. \tag{3.9}$$

Thus, by measuring the four transport coefficients, one can determine both the DOS effective mass and scattering parameter. In the non-parabolic case, equations (3.5) and (3.7) transform to

$$\alpha = 8\pi\left(\frac{\pi}{3}\right)^{5/3} \frac{k_B^2 T}{q\,h^2} \frac{1}{n^{2/3}} \left[m_d^*(r+1-\lambda)\right]_{E=E_F} \tag{3.10}$$

and

$$Q = |\alpha|\mu_H\left(\frac{r-1/2-\lambda}{r+1-\lambda}\right), \tag{3.11}$$

where

$$\lambda(E) = 2\gamma(E)\frac{d^2\gamma}{dE^2} = \frac{n}{m_d^*}\frac{dm_d}{dn}. \tag{3.12}$$

It is easy to show that m_d^* can be calculated from the measured data using the same equation (3.8), as in the parabolic case. The scattering parameter is now defined as

$$r = \frac{3}{2}\left(\frac{Q}{|\alpha|\mu_H - Q}\right) + \frac{1}{2} + \lambda. \tag{3.13}$$

To realize all the advantages offered by this method, we must have degenerate samples of a material in a wide range of carrier concentrations/Fermi level positions. Based on measurements of the four transport coefficients, we are able to obtain the dependence $m_d^* = f(n)$. If $m_d^*(n) = \text{const}$, the deviations from parabolicity are negligible, in this range of n and E_F, and, in subsequent analysis, we may reasonably use parabolic band theory. A substantial increase in m_d^* with carrier concentration indicates the need to use the more general non-parabolic band theory. Using the experimental dependence $m_d^* = f(n)$, with equations (2.20) and (2.21), we can reconstruct the function $\gamma(E)$ and, hence, $E(k)$. The scattering parameter data enable us to identify the dominant scattering mechanism and to monitor its changes as a function of carrier concentration.

It should be mentioned here that the empirically established correlation, $\alpha \sim N$, can be used to map the carrier concentration distribution over the sample area of a thin film.

Measurement of the local Seebeck coefficient, at various positions on the surface, by relocating the thermoprobe, is a non-destructive and simple method that may be applied to films of an arbitrary size and shape.

The method, coined *the method of four coefficients,* was first proposed and applied to studies of n-PbTe[9,10]and then used widely to study a variety of semiconductor and semimetals in bulk form. Our group at NREL has applied *the method of four coefficients* to thin-film TCO samples[11,12] using a specially designed instrument to measure the four coefficients on the same sample.

3.1 Experimental procedure

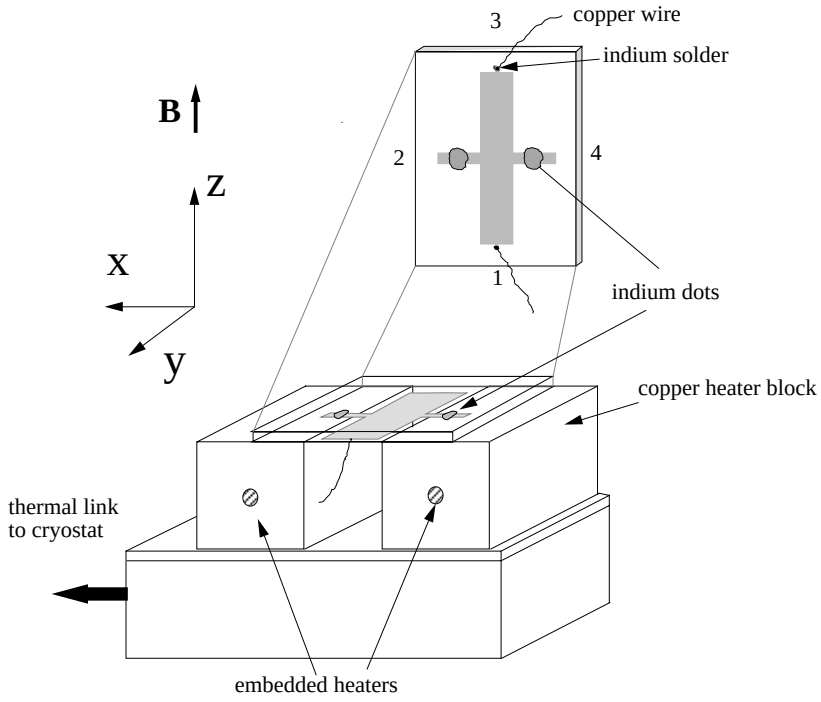

Figure 2. Transport coefficient instrument sample holder. Patterned thin-film sample is placed film-side down across heater blocks.

Our four-coefficient instrument for thin films has already been discussed in detail,[13] but a brief review of its operation is in order. Thin-film TCO samples are deposited on electrically insulating substrates and photolithographically etched to the pattern shown in Figure 2. As depicted in Figure 2, the film is placed film-side down across two copper heater blocks, with contacts 2 and 4 making ohmic contact with the heater blocks by an indium dot. Contacts 1 and 3 are indium-soldered to fine copper wire. The heater blocks are electrically isolated from each other, and each has a copper wire attached to it to make electrical contact to the film. The heater blocks have a differential thermocouple mounted between them to measure the temperature gradient across the sample. Heater block 2 has an additional embedded thermocouple for absolute temperature measurement.

The entire sample holder of Figure 2 is cooled by a closed-cycle helium cryostat for temperature-dependent measurements from 30 - 350 K.

To measure the four transport coefficients in equation (3.8), a specific data collection sequence is followed. Resistivity is measured by the van der Pauw method, i.e., biasing contacts 3 and 4 while measuring the voltage across contacts 1 and 2. The Hall coefficient is measured by biasing contacts 1 and 3 while a z-directed magnetic field (Figure 2) is applied and measuring the voltage across contacts 2 and 4. The thermoelectric, or Seebeck, coefficient is measured by establishing a temperature gradient between contacts 2 and 4 and measuring the voltage developed between the same two contacts. Finally, the Nernst coefficient is measured by maintaining the temperature gradient between contacts 2 and 4 while applying the z-directed magnetic field. A Nernst voltage is established between contacts 1 and 3.

3.2 Transport data and analysis: ZnO, Cd_2SnO_4

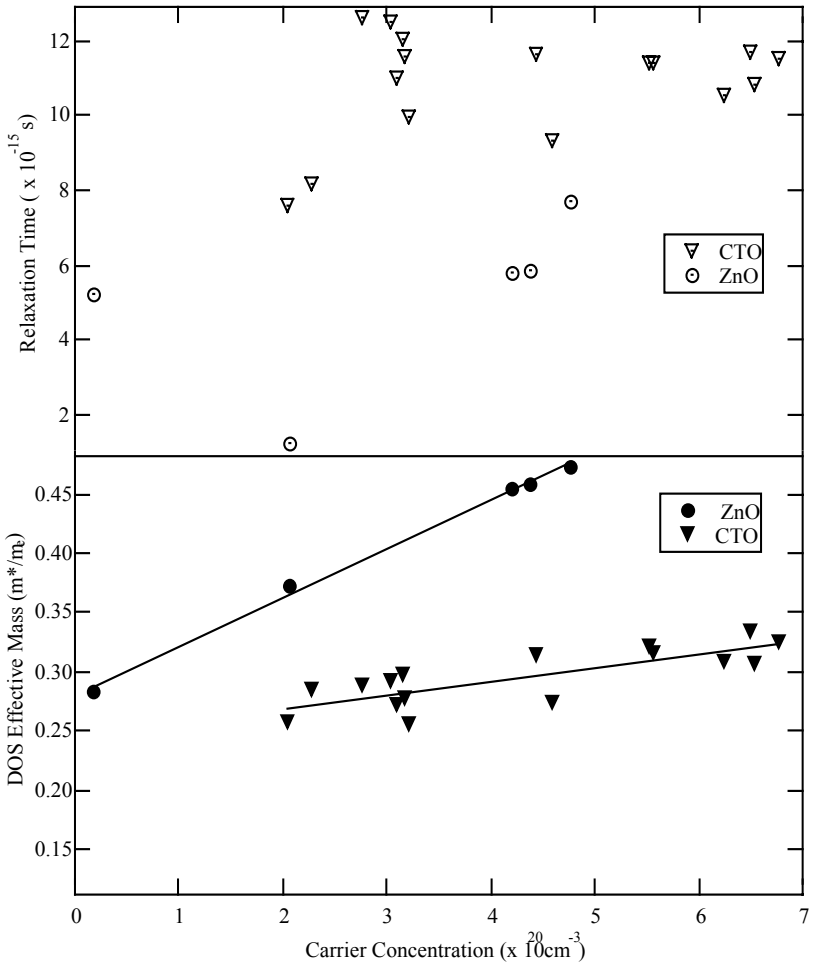

Figure 3. DOS effective mass and relaxation-time values for ZnO and Cd_2SnO_4 films versus carrier concentration.

The m_d^* values for both ZnO and CTO are not constant over the carrier concentration range probed for each of the films. This trend shows that the conduction bands for ZnO and CTO are non-parabolic in this carrier concentration range. ZnO shows a higher degree of non-parabolicity in the conduction band than does CTO. The upper graph of Figure 3 shows calculated relaxation times (equation (2.2)) based on the measured effective-mass values of Figure 3 and the measured Hall mobilities for both films. Several features of this graph are noteworthy. First, CTO films have relaxation times nearly twice that of the ZnO films. This difference accounts partially for mobilities in CTO being nearly 3 times larger than for ZnO. Second, the ZnO film with a carrier-concentration value of about 2 x 10^{20} cm^{-3} was purposely grown under non-ideal sputtering conditions to get a larger variation in carrier concentrations in the film set. The relaxation time for this film is very low compared with the other ZnO films in this data set. This fact correlates well with the idea that relaxation time is an *extrinsic* variable in thin-films that can be manipulated by process conditions. Note that the other ZnO films were grown under ideal conditions and that their relaxation times are approximately equal. CTO films have some of the longest relaxation times for TCO materials. This appears to be associated with the crystalline quality of this material after the standard annealing step that is used.[14]

Relaxation times are certainly a function of process conditions, but they are also influenced by the mechanism by which free carriers are scattered. As equation (3.13) suggests, *the method of four coefficients* may be used to calculate a scattering parameter, r, which is associated with specific scattering mechanisms. The scattering parameter is highly dependent on the curvature of the conduction band through the term λ. This term may be calculated from the lower graph in Figure 3 by equation (3.12).

Figure 4 shows the calculated scattering parameter values for the ZnO and CTO samples, along with the predicted trends in the scattering parameter for five scattering mechanisms. For the ZnO:Al samples, the measured scattering parameter lies near the trend expected for ionized impurity scattering (I.I.S.) with screening by free electrons. I.I.S. is predicted for these films, where aluminum is added to contribute an electron to the conduction band to dope the films n-type. The electron leaves behind an ionized aluminum atom that acts as an impurity scattering center. For the undoped ZnO, the scattering parameter lies most closely to the neutral impurity trend, presumably due to neutral interstitial Zn atoms. The CTO samples all show a scattering parameter most closely aligned with optical phonon scattering. Raman spectroscopy revealed several optical modes in the CTO samples. Hall mobility versus temperature data for all of the films involved in this study[4] correlate well with the scattering trends predicted by Figure 4.

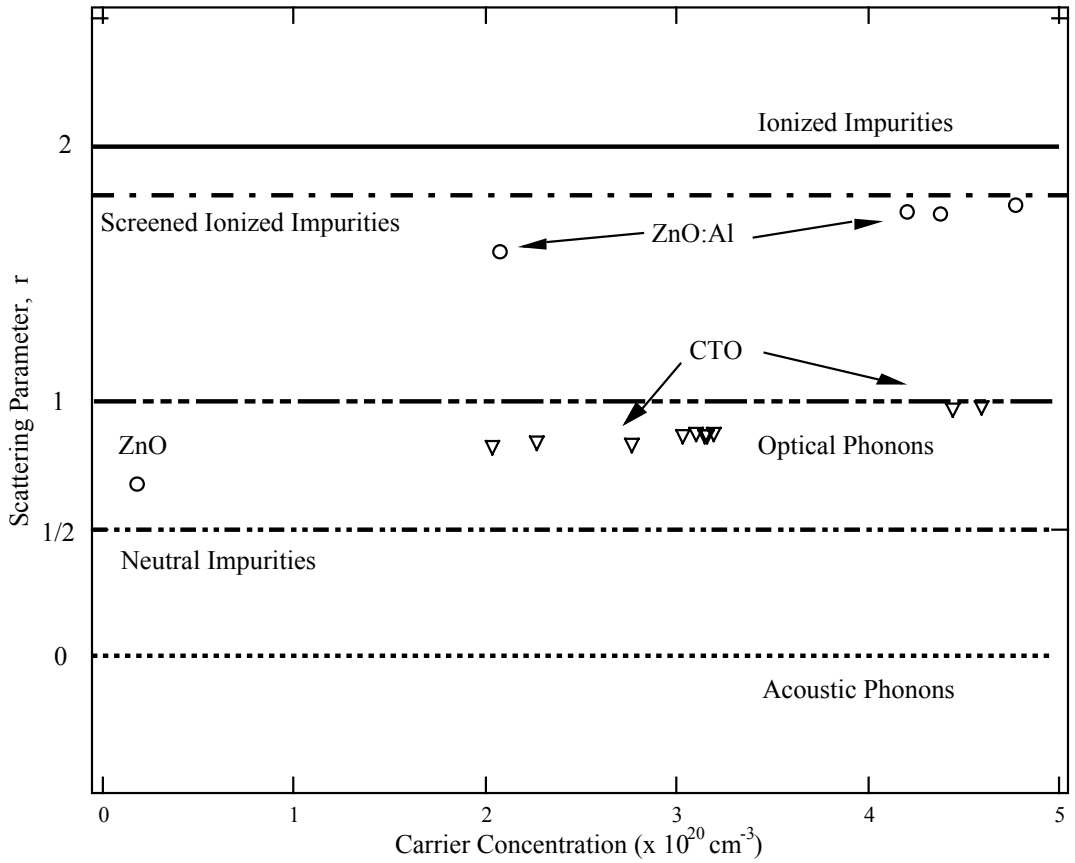

Figure 4. Scattering parameter versus carrier concentration for ZnO and CTO films.

Returning to Figure 3 and the relaxation-time values for the samples, we see that the scattering mechanisms revealed in Figure 4 may help understand why CTO has a much longer relaxation time. CTO predominantly is limited by phonon-like scattering, whereas ZnO and ZnO:Al suffer from impurity-type scattering. Phonon scattering represents an intrinsic mechanism that cannot be overcome by adjusting growth parameters, whereas impurity scattering theoretically could be controlled by proper growth techniques. We conclude that CTO has a long relaxation time because it is relatively defect-free, and thus, mobility-limited by an intrinsic phonon scattering mechanism.

Much more information may be gleaned from the transport coefficient data for these films than space permits, but the interested reader is referred to the following references for further details.[4,12-15]

4. Optical characterization (ultra-high frequency electron transport)

The high electrical conductivity in metals and heavily doped semiconductors, and its dependence on frequency, significantly influences the optical properties of these materials and, in particular, the transmittance and reflectance spectra. The electrical conductivity is a complex value and depends on frequency of the a.c. electric field. It is given by

$$\sigma(\omega) = \frac{\sigma_0}{1 - i\omega\tau}, \tag{4.1}$$

where σ_0 is the stationary (DC) conductivity, which is defined as

$$\sigma_0 = e^2 n \tau / m_c^* . \tag{4.2}$$

The real and imaginary parts of the dielectric permittivity are described by equations (4.3) and (4.4).

$$\mathrm{Re}\,\varepsilon = \varepsilon' = N^2 - k^2 = \varepsilon_\infty \left(1 - \frac{\omega_p^2}{\omega^2 - \omega_c^2} \right), \tag{4.3}$$

and

$$\mathrm{Im}\,\varepsilon = \varepsilon'' = 2Nk = \varepsilon_\infty \left(\frac{\omega_p^2 \omega_c}{\omega(\omega^2 + \omega_c^2)} \right). \tag{4.4}$$

N and *k* are the refractive index and extinction coefficient, respectively, and ε_∞ is the "high- frequency" dielectric permittivity due to the bound electrons. Two characteristic frequencies, ω_p and ω_c, are totally defined by the free carriers. The plasma frequency, ω_p, is related to the carrier concentration and conductivity effective mass by equation (2.7). The collision frequency, ω_c, is the reciprocal of the relaxation time, $\omega_c = 1/\tau$,

When the frequency of an electromagnetic wave, ω, decreases so that it is close to ω_p, reflectance and transmittance of the material change dramatically. If $\omega_c << \omega_p$, then, to a first approximation,

$$\varepsilon \approx \varepsilon' = \varepsilon_\infty \left(1 - \omega_p^2 / \omega^2\right). \tag{4.5}$$

When ε is real and negative ($\omega < \omega_p$), the solutions to the wave equation decay exponentially in the material; i.e., no radiation can propagate. Thus, at $\omega = \omega_p$, a sharp increase in reflectivity, known as the "plasma reflectivity edge," should be observed. For practical conductors, ω_c/ω_p is usually not insignificant; therefore, reflectance does not change so rapidly when the frequency approaches ω_p. The analysis of the measured optical spectra (e.g., by, spectrophotometry or ellipsometry) allows the plasma and collision frequencies to be determined.

Based on the plasma frequency and Hall carrier concentration data, it is possible to calculate the conductivity effective mass, m_c^*, using equation (2.5). Comparison of m_c^* with m_d^* (see Section 3) provides guidance about the shape of the constant-energy

surfaces. The measured dependence, $m_c^*(n)$, establishes the non-parabolicity and reconstruction of $\gamma(E)$ and $E(k)$ dependencies in the same way as $m_d^*(n)$.

Based on the m_c^* and ω_c data, one can calculate the *optical mobility* defined as

$$\mu_0 = \frac{e\tau}{m_c^*} = \frac{e}{m_c^* \omega_c}, \tag{4.6}$$

which is not necessarily the same as the Hall mobility. Their difference, if any, provides guidance about some peculiarities in the electronic properties of the films (see Section 5). The empirically established dependence, $\omega_p(n)$, for a particular material provides an alternative to the Hall effect method for measuring carrier concentration and its uniformity over the thin-film area. Multi-angle spectroscopic ellipsometry, with appropriate modeling of the raw data, provides a unique option to test the uniformity of n and μ (via ω_p and ω_c) over the film thickness.[17]

5. Investigation of the electrical properties of grain boundaries

There is usually a significant difference between the resistivity of single crystals and polycrystalline samples of the same semiconductor with the same carrier concentration. This is usually attributed to the influence of grain boundaries, and it is customary to treat the problem in terms of grain-boundary scattering. This terminology is not always correct and sometimes can be misleading.

Indeed, grain boundaries disturb the translation symmetry of the crystal and inevitably cause free-carrier scattering. However, grain-boundary scattering coexists with scattering by phonons, point defects, and dislocations, and the total scattering rate is the sum of the individual rates. The contribution of grain-boundary scattering is significant only if the grain size, d, is comparable to the mean free path, l, as determined by all scattering mechanisms. In typical polycrystalline thin TCO films the l value estimated based on the mobility and carrier concentration is rather small: $l \sim 100$ Å, while $d \sim 1000$ Å.

Thus, we have to use a different approach to the problem. Namely, we must regard a TCO polycrystalline film as having two phases. One of these is the material inside the grains (bulk material), and the other is that at grain boundaries. The equivalent electrical circuit of the sample can be constructed as a series connection of resistors, R_B and R_{GB}, representing bulk material and grain boundaries, respectively. When measuring the DC resistance of the film, we obtain the sum of these two types of resistors. Thus, the measured bulk resistivity, ρ, relates to the real resistivity in the grain bulk, ρ_B, as

$$\rho = \rho_B \left(1 + R_{GB} / R_B\right). \tag{5.1}$$

The first of the experimental methods we discuss in this section to estimate the contribution of the grain boundaries to the measured resistivity/sheet resistance of the polycrystalline film is based on a comparison of the optical and Hall mobilities.

Scattering in the grain bulk, in TCO films, dominates the collision frequency, ω_c, because $d >> l$. Thus, the optical mobility, defined by equation (4.6), is close to the real drift mobility in the grain bulk. The Hall mobility, given by equation (3.4), is determined from Hall coefficient and DC conductivity measurements: $\mu_H = R_H / \rho$. Hence, the measured Hall mobility due to the influence of grain boundaries may differ significantly from the real mobility in the grain bulk. If we assume that the Hall factor, $A_H > 1$, then, using equations (4.5) and (5.1), we obtain equation (5.2), which enables an estimate of the grain-boundary contribution to the resistivity to be made.

$$\frac{R_{GB}}{R_B} = \frac{\mu_0}{\mu_H} - 1. \tag{5.2}$$

This method was applied to the evaluation of the grain-boundary contribution in several TCOs. It was found that, for the relatively high carrier-concentration materials, ($n > 3x10^{20}cm^{-3}$), $\mu_0 \approx \mu_H$; that is, $R_{GB} / R_B << 1$.[16,17] On the other hand, films with much lower carrier concentrations demonstrated a considerable difference between μ_o and μ_H, thereby indicating the impact of grain boundaries.

These results are consistent with a model widely used to explain the enhanced resistance of grain boundaries.[18-20] The electrical charge located at grain boundaries, due to trapping of majority carriers by the electron states, creates a potential barrier for free carriers and increases the resistance of the grain-boundary regions. With increasing doping level, the amount of the trapped charge also increases, as does the height of the potential barrier. As the doping level continues to increase, eventually all the grain-boundary states are filled with trapped carriers and the charge cannot increase any more. With further increase in carrier concentration, the space-charge density in the depletion region increases, leading to a reduction in the height and width of the potential barrier and making it transparent to carrier tunneling. Moreover, for a very high doping level, the potential barrier is well below the Fermi level and the electrons pass over the barrier without being greatly perturbed by it.[21,22]

Application of the method discussed above is limited to films with a high doping level, for which the plasma reflection edge is within the visible or near-infrared range. The method we discuss below does not suffer from this limitation. Indeed, the lower the doping level and the higher the grain-boundary resistance, the better. This method is based on using impedance spectroscopy. In the AC equivalent circuit of the films, the grain-boundary regions may be represented as resistors, R_{GB}, in parallel with capacitors, C_{GB}. The latter arises from the semi-insulating properties of the depleted region adjacent to the grain boundary. The measured DC (low-frequency) resistance of the film is $R = R_{GB} + R_B$, in which R_B represents the contribution of the bulk material. At high frequency, R_{GB} is shunted by C_{GB}, and R tends to the R_B. By fitting the measured frequency-dependent impedance to the appropriate electrical model, one can determine all three parameters and even estimate the distribution of the grain boundary electrical parameters. Measuring R_{GB} over a range of temperatures and modeling with various transport mechanisms across the potential barrier provide an estimate of the potential

barrier height.[19,23] The measured value of C_{GB} enables an estimate to be made of the doping level in the vicinity of the grain boundary.[26,27] This can be significantly different from that in the grain bulk. Measurement of R_{GB} as a function of applied bias enables the grain-boundary density of states and its dependence on the deposition technique to be calculated.[25] Post-deposition treatment, carrier type, and concentration may also be evaluated. Recently, impedance spectroscopy was successfully used in studies of the electronic properties of grain boundaries in CdTe thin films used in photovoltaic cells.[23,26]

6. Summary

In this paper, we have reviewed the need to put the study of TCOs on a more scientific basis than is presently the case. In particular, it is necessary to learn more about the transport properties of these materials and to have some knowledge of their electronic band structure. These studies are essential to make calculations of the ultimate properties of the materials, and thereby, to determine if a specific material has the potential to meet the demands for TCOs as the associated applications evolve. We have reviewed *the method of four coefficients* and have demonstrated its utility in measuring the properties of electrons in TCOs and, in particular, to assessing the dominant scattering mechanism that limits both electrical and optical properties. The extension of the analysis to non-parabolic bands was demonstrated and the appropriate background theory was provided, although this was first elaborated over 30 years ago, this is the first time the technique has been applied to TCO thin films.

In the fourth section, we discussed the measurement of the optical properties of TCOs and the implications of comparisons of these with the electrical measurements. Finally, we reviewed techniques used to characterize the grain boundaries in TCO films. It is concluded that for materials with very high degeneracy, the grain boundaries do not present a significant obstacle to electrons as they cross from one grain to another. The limiting factor on the mobility of the materials appears, therefore, to depend on the quality of the material within the grains themselves.

References

[1]E. Putley, *The Hall Effect and Related Phenomena* (Butterworths, London, 1960).
[2]R. A. Smith, *Semiconductors* (Cambridge University Press, London and New York, 1956).
[3]L. Burstein, Phys. Rev. **93**, 632-633 (1954).
[4]B. M. Askerov, *Electron Transport Phenomena in Semiconductors* (World Scientific, Singapore, 1994).
[5]I. A. Chernik, V. Kaydanov, and E. P. Ishutinov, Soviet Physics - Semiconductors **2**, 825-829 (1969).
[6]I. A. Chernik, V. I. Kaidanov, M. I. Vinogradova, and N. V. Kolomoets, Soviet Physics - Semiconductors **2**, 645-651 (1969).
[7]J. Kolodziejchak and S. Zhukotynski, Phys. Stat. Sol. (a) **5**, 145-158 (1964).
[8]W. Zawadzki and J. Kolodziejchak, Phys. Stat. Sol. **6**, 419-428 (1964).
[9]M. K. Zhitinskaya, V. I. Kaidanov, and I. A. Chernik, Soviet Physics-Solid State **8**, 246-247 (1966).
[10]S. Zukotynski and J. Kolodziejczak, Phys. Stat. Sol. **19**, 51-54 (1967).
[11]W. P. Mulligan, Ph.D. Thesis, Colorado School of Mines, 1997.
[12]D. L. Young, T. J. Coutts, V. I. Kaydanov, and W. P. Mulligan, J. Vac. Sci. Technol., to be published (2000).
[13]D. L. Young, T. J. Coutts, and V. I. Kaydanov, Rev. Sci. Inst. **71**, 462-466 (2000).
[14]T. J. Coutts, D. L. Young, X. Li, and X. Wu, J. Vac. Sci. Technol., to be published (2000).
[15]D. L. Young, Ph.D. Thesis, The Colorado School of Mines, 2000.
[16]A. Al-Kaoud, T. Wen, A. S. Gilmore, V. Kaydanov, T. R. Ohno, C. Wolden, L. Feng, and J. Xi, in *Atmospheric Pressure Chemical Vapor Deposition of SnO_2: Processing and Properties*, Denver, Colorado, 1998 (American Institute of Physics), p. 212-217.
[17]A. M. Al-Kaoud, Ph.D. Thesis, Colorado School of Mines, 1999.
[18]H. F. Matare, *Defect Electronics in Semiconductors* (Wiley Interscience, New York, 1971).
[19]R. H. Bube, Annual Reviews in Materials Science **5**, 201-224 (1975).
[20]H. J. Leamy, H. J. Pike, and C. H. Seager, in *Grain Boundaries in Semiconductors*, Amsterdam, 1982 (North Holland).
[21]T. S. Gudkin and V. Kaydanov, Soviet Physics - Semiconductors **8**, 1453-1454 (1975).
[22]B. M. Gol'tsman, Z. M. Dashevsky, V. I. Kaydanov, and N. V. Kolomoets, *Thin Film Thermoelements: Physics and Applications (in Russian)* (Nauka, Moscow, 1985).
[23]L. M. Woods, D. H. Levi, V. Kaydanov, G. Y. Robinson, and R. K. Ahrenkiel, in *Electrical Characterization of the CdTe Grain-Boundary Properties from as-Processed CdTe/Cds Solar Cells*, Vienna, Austria, 1998 (Office for Official Publications of the European Community), p. 1043-1046.
[24]G. E. Pike and C. H. Seager, J. Appl. Phys. **50**, 3414-3422 (1979).
[25]C. H. Seager and G. E. Pike, Appl. Phys. Lett. **37**, 747-749 (1980).
[26]A. S. Gilmore, V. Kaydanov, U. Laor, A. Gupta, T. R. Ohno, and B. McCandless, in *Ac Characterization of the Grain Boundary Electronic Properties in CdTe Thin Films*, Proc. NCPV Prog. Rev. Meeting 2000, Denver, Colorado, 2000 (American Institute of Physics), p. 259-260.
[27]T. P. Thorpe, A. L. Fahrenbruch, and R. H. Bube, J. Appl. Phys. **60**, 3622-3630 (1986).

REPORT DOCUMENTATION PAGE

Form Approved
OMB NO. 0704-0188

Public reporting burden for this collection of information is estimated to average 1 hour per response, including the time for reviewing instructions, searching existing data sources, gathering and maintaining the data needed, and completing and reviewing the collection of information. Send comments regarding this burden estimate or any other aspect of this collection of information, including suggestions for reducing this burden, to Washington Headquarters Services, Directorate for Information Operations and Reports, 1215 Jefferson Davis Highway, Suite 1204, Arlington, VA 22202-4302, and to the Office of Management and Budget, Paperwork Reduction Project (0704-0188), Washington, DC 20503.

1. AGENCY USE ONLY (Leave blank)	2. REPORT DATE	3. REPORT TYPE AND DATES COVERED
	October 2000	Conference Paper

4. TITLE AND SUBTITLE
Studies of Band Structure and Free-Carrier Scattering in Transparent Conducting Oxides Based on Combined Measurements of Electron Transport Phenomena

5. FUNDING NUMBERS
C
TA: PV004701

6. AUTHOR(S)
V.I. Kaydanov, T.J. Coutts, and D.L. Young

7. PERFORMING ORGANIZATION NAME(S) AND ADDRESS(ES)

8. PERFORMING ORGANIZATION REPORT NUMBER

9. SPONSORING/MONITORING AGENCY NAME(S) AND ADDRESS(ES)
National Renewable Energy Laboratory
1617 Cole Blvd.
Golden, CO 80401-3393

10. SPONSORING/MONITORING AGENCY REPORT NUMBER
NREL/CP-520-29064

11. SUPPLEMENTARY NOTES

12a. DISTRIBUTION/AVAILABILITY STATEMENT
National Technical Information Service
U.S. Department of Commerce
5285 Port Royal Road
Springfield, VA 22161

12b. DISTRIBUTION CODE

13. ABSTRACT *(Maximum 200 words)*

Experimental methods are discussed for studying band structure, effective mass, and other electronic properties relevant to mobility, including scattering mechanisms, relaxation time, and the influence of grain boundaries (GBs) in polycrystalline transparent conducting oxide (TCO) films. Impedance spectroscopy permits evaluation of the GB potential barrier height and density-of-states. These studies enable an estimate of the limiting mobility achievable for practical transparent conducting oxides to be made. The equipment for measurement of the four transport coefficients is discussed, and examples of its application to films of ZnO, SnO2, and Cd2SnO4 are given.

14. SUBJECT TERMS
band structure ; effective mass ; scattering mechanisms ; optical characterization ; Nernst-Ettingshausen coefficients ; Fermi level ; spectroscopy permits evaluation ; grain boundaries (GBs) ; polycrystalline films.

15. NUMBER OF PAGES

16. PRICE CODE

17. SECURITY CLASSIFICATION OF REPORT	18. SECURITY CLASSIFICATION OF THIS PAGE	19. SECURITY CLASSIFICATION OF ABSTRACT	20. LIMITATION OF ABSTRACT
Unclassified	Unclassified	Unclassified	UL